

## Supporting Information for

### *Enhanced Phosphate Removal by Nanosized Hydrated La(III) Oxide Confined in Crosslinked Polystyrene Networks*

Yanyang Zhang, Bingcai Pan\*, Chao Shan, Xiang Gao

State Key Laboratory of Pollution Control and Resource Reuse, School of the Environment,  
Nanjing University, Nanjing 210023, China

\*To whom correspondence should be addressed

E-mail: [bcpan@nju.edu.cn](mailto:bcpan@nju.edu.cn) (B. Pan)

Tel: +86-25-8968-0390

This file contains 14 pages, including Appendix S1-S4, Table S1-S5, and Figure S1-S8.

## Appendix S1

Thermogravimetric analysis of  $\text{LaPO}_4 \cdot x\text{H}_2\text{O}$ , heat from 25°C to 750°C at 20°C/min. The water content of  $\text{LaPO}_4 \cdot x\text{H}_2\text{O}$  was determined by calculation as follows:

$$x\text{H}_2\text{O} = \frac{M_{\text{initial}} - M_{\text{LaPO}_4}}{M_{\text{H}_2\text{O}}}; M_{\text{initial}} = \frac{M_{\text{LaPO}_4}}{(1 - \text{weightloss})}$$

**Table S1 Thermogravimetric analysis of model compound  $\text{LaPO}_4 \cdot x\text{H}_2\text{O}$**

Temperature °C	Weight loss %	$x\text{H}_2\text{O}$
25-750	10.20-13.80	1.47-2.08

## Appendix S2

Equations used in this study are Langmuir model (1), Freundlich model (2), Double Langmuir model (3), Sips model (4), Pseudo-first-order model (5) and Pseudo-second-order model (6)

$$q_e = q_m \frac{k_L c_e}{1 + k_L c_e} \quad (1)$$

$$q_e = K_F C_e^{1/n} \quad (2)$$

Where  $q_m$  (mg/g) represents the adsorption capacity and  $K_L$  is the Langmuir constant.  $K_F$  (L/mg) represents the heterogeneity of the sorbent and  $n$  is the Freundlich constant.

$$q_e = q_1 \frac{k_1 c_e}{1 + k_1 c_e} + q_2 \frac{k_2 c_e}{1 + k_2 c_e} \quad (3)$$

Where  $q_1$  and  $q_2$  (mg/g) represents the adsorption capacity of site 1 and 2, and  $k_1$  and  $k_2$  (L/mg) are the Double Langmuir constants

$$q_e = \frac{q_m (b c_e)^\beta}{1 + (b c_e)^\beta} \quad (4)$$

Where  $q_m$  and  $b$  are the same as  $q_m$  and  $K_L$  in the Langmuir model,  $\beta$  is similar to  $K_F$  in the Freundlich model

$$q_t = q_e (1 - e^{-k_1 t}) \quad (5)$$

$$q_t = \left( \frac{1}{q_e} + \frac{1}{k_2 q_e^2} t^{-1} \right)^{-1} \quad (6)$$

Where  $q_e$  and  $q_t$  are the adsorption amounts extracted in equilibrium and at time  $t$  respectively, and  $k_1$  and  $k_2$  are the pseudo-first-order and pseudo-second-order constant, respectively

**Table S2 The pseudo-first-order, pseudo-second-order kinetic model parameters for phosphorus adsorption onto La-201 in sulfate free solution and in background solution containing 500 mg/L sulfate.**

Background solution	Pseudo-first-order model			Pseudo-second-order model		
	$q_e$ mg · g <sup>-1</sup>	$k_1$ min <sup>-1</sup>	$R^2$	$q_e$ mg · g <sup>-1</sup>	$k_2$ mg · g <sup>-1</sup> · min <sup>-1</sup>	$R^2$
sulfate free	52.95	0.68	0.982	56.92	0.017	0.994
500 mg/L	$q_e$	$k_1$	$R^2$	$q_e$	$k_2$	$R^2$

sulfate	$\text{mg}\cdot\text{g}^{-1}$	$\text{min}^{-1}$		$\text{mg}\cdot\text{g}^{-1}$	$\text{mg}\cdot\text{g}^{-1}\cdot\text{min}^{-1}$	
	45.01	0.11	0.969	51.55	0.0023	0.988

---

**Table S3 Comparison of phosphorus adsorption capacity and La usage efficiency for different La-based materials**

Materials	pH	La content %	$q_m$ mg/g	Molar ratio P/La	Ref
Lanthanum-treated lignocellulosic	6.39, 6.05	2.75, 4.20	6.54, 10.88	<b>1.77, 2.58</b>	1
La(III)-chelex resin	3.1	12.38	3.04	<b>0.11</b>	2
Nanocrystalline La <sub>2</sub> O <sub>3</sub>	-	-	57.80	-	3
Synthesized Lanthanum hydroxide	-	-	107.53	-	4
Zeolite/lanthanum hydroxide	-	21.80	71.94	<b>1.48</b>	5
Lanthanum hydroxide doped activated carbon fiber	-	5.29	15.30	<b>1.30</b>	6
Lanthanum loaded mesoporous silica SBA-15	-	23.29	45.63	<b>0.</b>	7
Lanthanum modified macroporous silica foams	-	32.3	70.43	<b>0.98</b>	8
La(OH) <sub>3</sub> modified exfoliated vermiculites	5.0	41.55	79.60	<b>0.85</b>	9
La-201	6.7	15.80	113.64	<b>1.43</b>	This study

#### Appendix S3

The molar P/La ratio of the reference adsorbents was calculated on the basis of their maximum adsorption capacity and La content, which is possibly higher than the real values because the role of the host in phosphate adsorption was not excluded. As for La-201 in this study, since the host D-201 could adsorb phosphate considerably (Table S4), we deliberately excluded its contribution to phosphate adsorption by employing the background sulfate solution (Table S5) and the molar P/La ratio 1.43 reflected the real La usage.

**Table S4 Double Langmuir adsorption isotherm parameters for phosphorus adsorption onto La-201 at 25°C in sulfate free solution.**

Double Langmuir				
$q_1$ mg/g*	$k_1$ L/mg P	$q_2$ mg P/g*	$k_2$ L/mg P	$R^2$
69.78	0.017	43.86	11.25	0.991

**Table S5 Langmuir and Freundlich adsorption isotherm parameters for phosphorus adsorption onto La-201 at 25°C at the presence of 500 mg/L sulfate**

Langmuir				Freundlich	
$q_m$ mg/g*	$K_L$ L/mg P	$R^2$	$n$	$K_F$ L/mg	$R^2$
318.37	1.05	0.980	7.81	173.93	0.766

Langmuir				Freundlich	
$q_m$ mg/g#	$K_L$ L/mg P	$R^2$	$n$	$K_F$ L/mg	$R^2$
50.30	1.05	0.980	7.81	27.48	0.766

\* mg P/g La; # mg P/g La-201

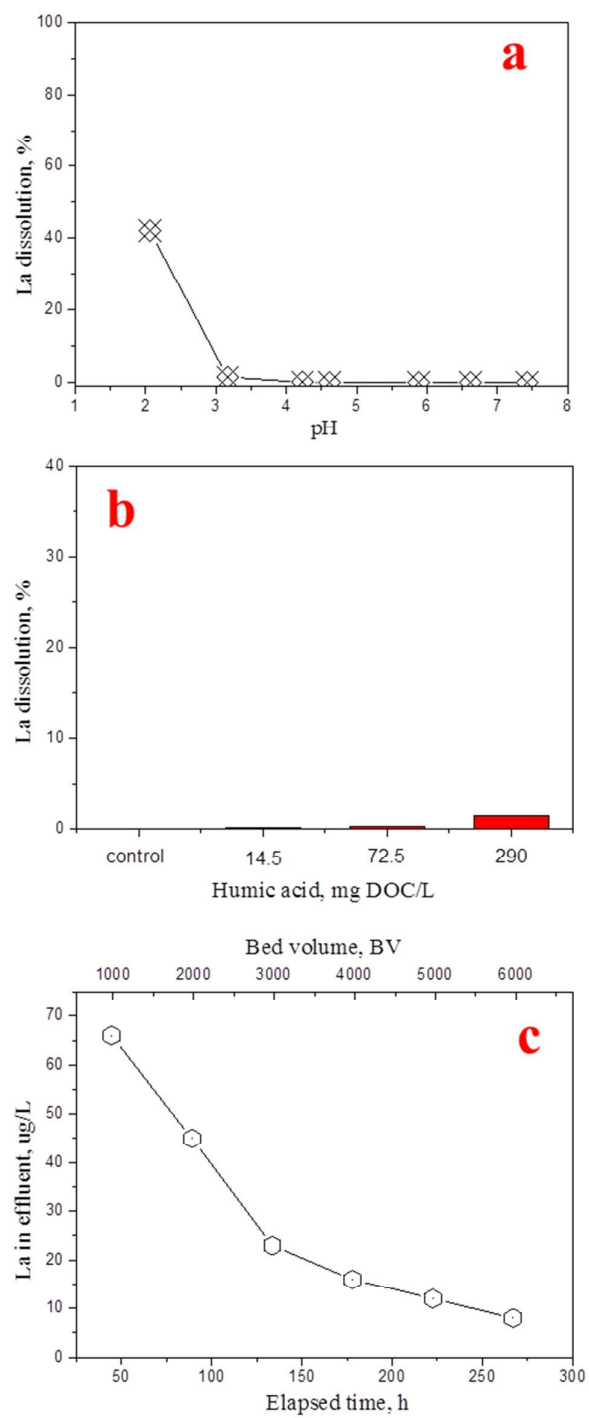


Figure S1 La dissolution from La-201 (a) at varying pH, (b) in the presence of different HA concentration for 20 days, (c) during column adsorption

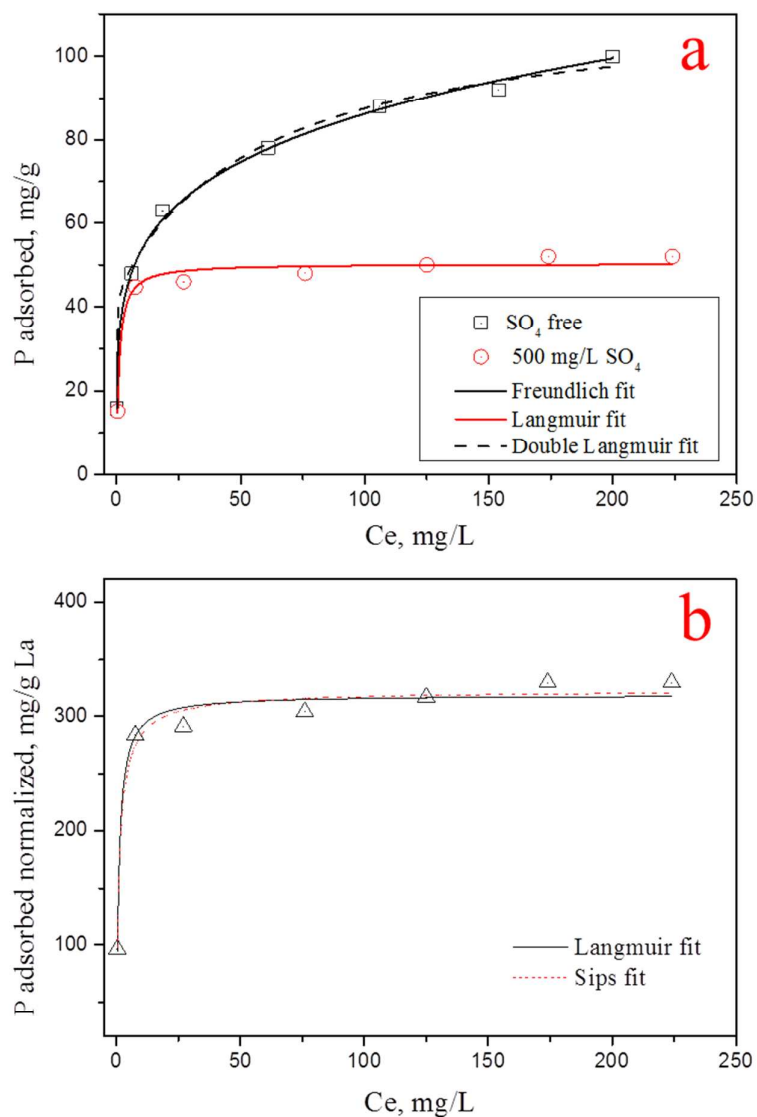


Figure S2 Phosphate adsorption isotherm onto La-201 in the background solution of sulfate free or sulfate at 25°C (a). Normalized adsorption isotherm in background sulfate solution (b) (S/L ratio, 0.5 g/L; time, 96 h).



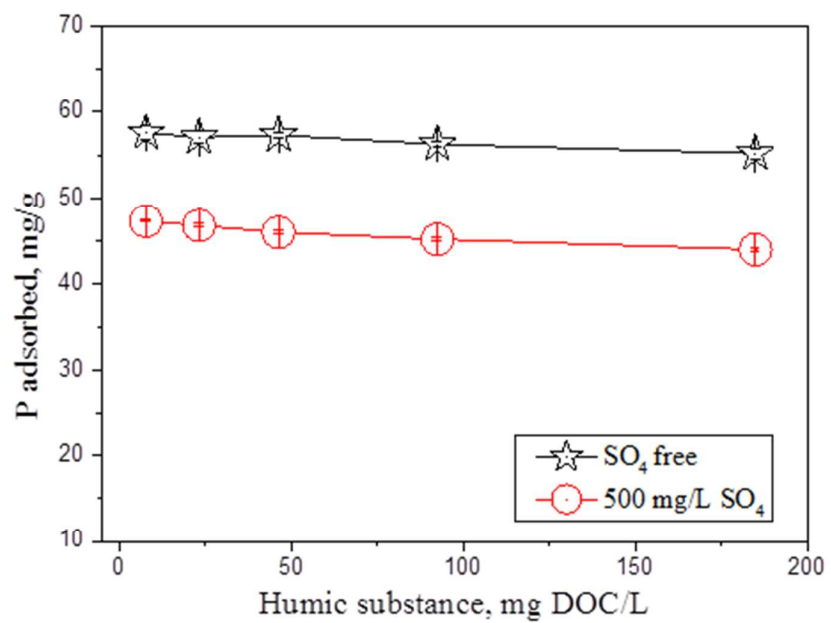


Figure S3 Effect of humic acid on the phosphate adsorption by using La-201 (25°C, pH=6.7, adsorbent dosage = 0.5 g/L, reaction time: 96 h,  $C_0$ =30 mg P/L).

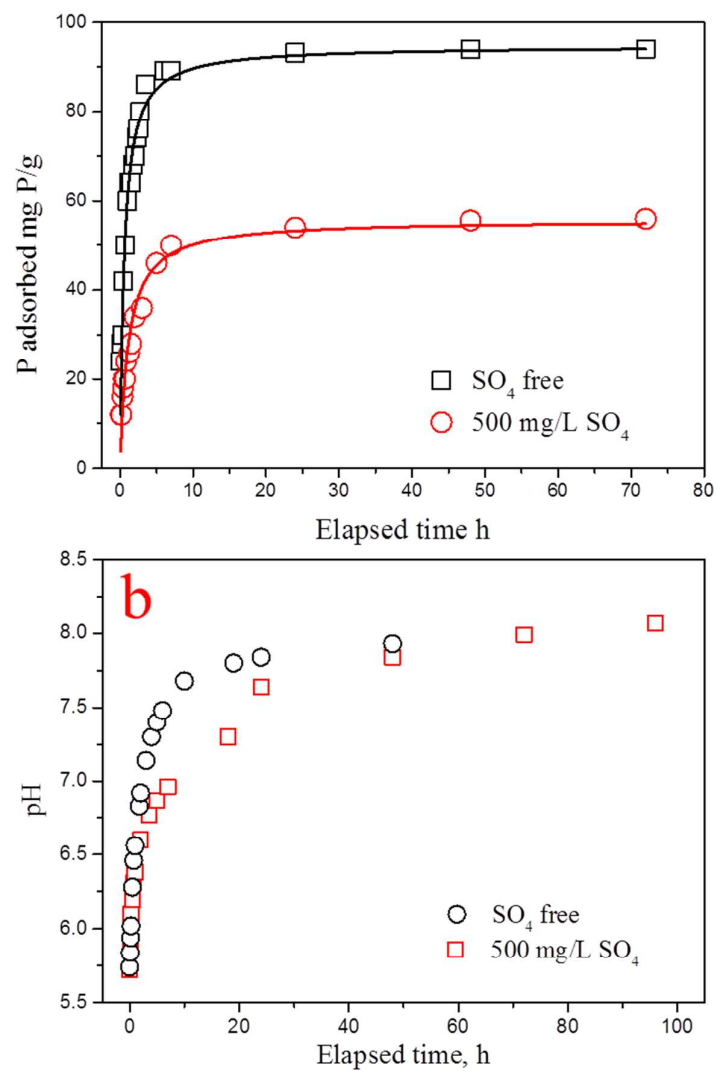


Figure S4 Phosphate uptake kinetics ( $C_0=150$  mg P/L, *a*) and pH variation (*b*) in the background of sulfate and sulfate free solution (25°C,  $C_0=30$  mg P/L, adsorbent dosage = 0.5 g/L).

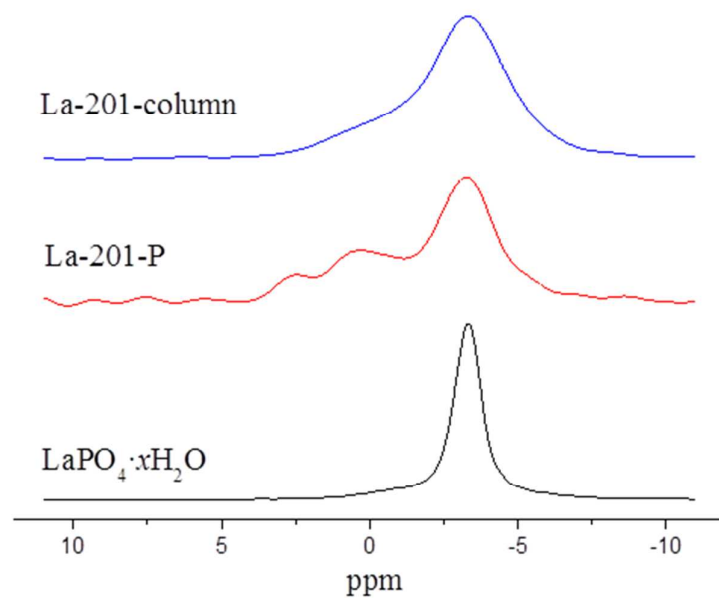


Figure S5  $^{31}\text{P}$  MAS NMR spectra of La-201 after P saturation and after column adsorption, and  $\text{LaPO}_4 \cdot x\text{H}_2\text{O}$ .

#### Appendix S4

The NMR spectrum of La-201-P has two additional resonance at  $\delta(^{31}\text{P}) = 0.33$  and  $2.47$  ppm, which could reflect P adsorbed by ammonium groups and P species formed on the surface of  $\text{LaPO}_4 \cdot x\text{H}_2\text{O}$ <sup>10,11</sup>, respectively.

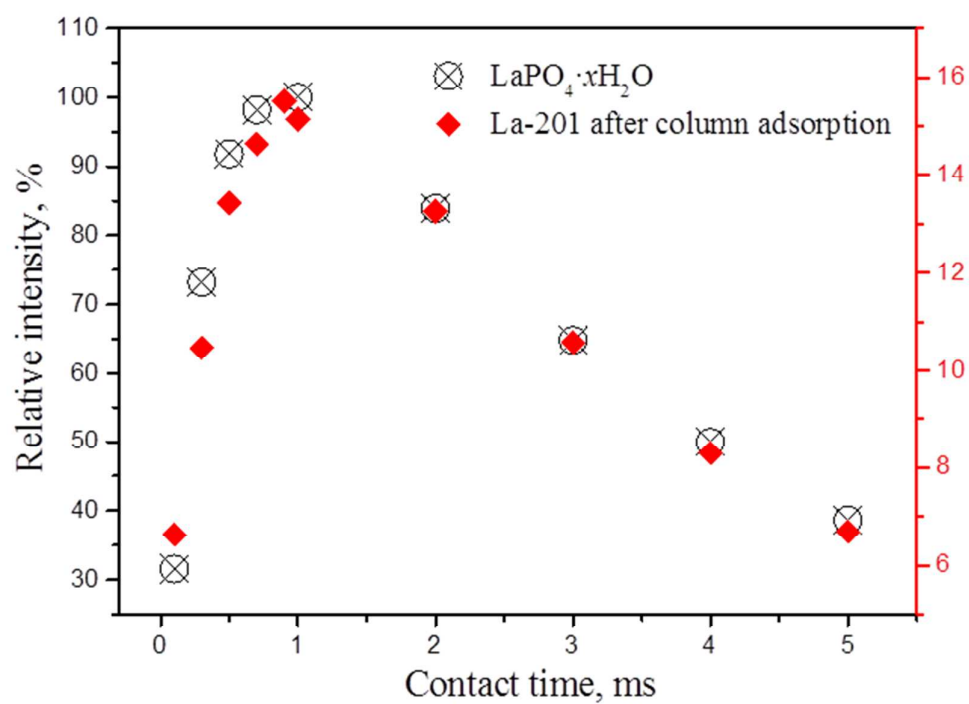


Figure S6 Relative intensity of  $\text{LaPO}_4 \cdot x\text{H}_2\text{O}$  (left  $Y$  axis) and La-201 after column adsorption (right  $Y$  axis) determined from  $^{31}\text{P}\{^1\text{H}\}$  CP MAS NMR experiments as a function of contact time. The intensities are normalized relative to the most intense value for  $\text{LaPO}_4 \cdot x\text{H}_2\text{O}$ .

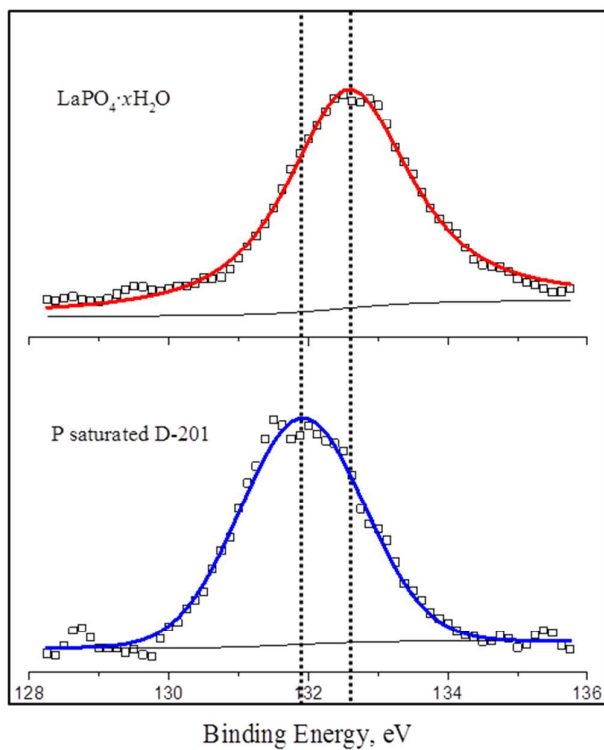


Figure S7 P2p XPS scan spectra of  $\text{LaPO}_4 \cdot x\text{H}_2\text{O}$  and P saturated D-201

## LITERATURE CITED

- (1) Shin, E. W.; Karthikeyan, K. G.; Tshabalala, M. A. Orthophosphate sorption onto lanthanum-treated lignocellulosic sorbents. *Environ Sci Technol* **2005**, *39*, 6273-6279.
- (2) Wu, R. S. S.; Lam, K. H.; Lee, J. M. N.; Lau, T. C. Removal of phosphate from water by a highly selective La(III)-chelex resin. *Chemosphere* **2007**, *69*, 289-294.
- (3) Long, Y. L.; Yang, J.; Li, X. C.; Huang, W. Y.; Tang, Y.; Zhang, Y. M. Combustion synthesis and stability of nanocrystalline La<sub>2</sub>O<sub>3</sub> via ethanolamine-nitrate process. *J Rare Earth* **2012**, *30*, 48-52.
- (4) Xie, J.; Wang, Z.; Lu, S. Y.; Wu, D. Y.; Zhang, Z. J.; Kong, H. N. Removal and recovery of phosphate from water by lanthanum hydroxide materials. *Chem Eng J* **2014**, *254*, 163-170.
- (5) Xie, J.; Wang, Z.; Fang, D.; Li, C. J.; Wu, D. Y. Green synthesis of a novel hybrid sorbent of zeolite/lanthanum hydroxide and its application in the removal and recovery of phosphate from water. *J Colloid Interf Sci* **2014**, *423*, 13-19.
- (6) Zhang, L.; Zhou, Q.; Liu, J. Y.; Chang, N.; Wan, L. H.; Chen, J. H. Phosphate adsorption on lanthanum hydroxide-doped activated carbon fiber. *Chem Eng J* **2012**, *185*, 160-167.
- (7) Yang, J.; Zhou, L.; Zhao, L. Z.; Zhang, H. W.; Yin, J. N.; Wei, G. F.; Qian, K.; Wang, Y. H.; Yu, C. Z. A designed nanoporous material for phosphate removal with high efficiency. *J Mater Chem* **2011**, *21*, 2489-2494.
- (8) Yang, J.; Yuan, P.; Chen, H. Y.; Zou, J.; Yuan, Z. G.; Yu, C. Z. Rationally designed functional macroporous materials as new adsorbents for efficient phosphorus removal. *J Mater Chem* **2012**, *22*, 9983-9990.
- (9) Huang, W. Y.; Li, D.; Liu, Z. Q.; Tao, Q.; Zhu, Y.; Yang, J.; Zhang, Y. M. Kinetics, isotherm, thermodynamic, and adsorption mechanism studies of La(OH)<sub>3</sub>-modified exfoliated vermiculites as highly efficient phosphate adsorbents. *Chem Eng J* **2014**, *236*, 191-201.
- (10) Sorensen, D. R.; Nielsen, U. G.; Skou, E. M. Solid state P-31 MAS NMR spectroscopy and conductivity measurements on NbOPO<sub>4</sub> and H<sub>3</sub>PO<sub>4</sub> composite materials. *J Solid State Chem* **2014**, *219*, 80-86.
- (11) Lucas, S.; Champion, E.; Bregiroux, D.; Bernache-Assollant, D.; Audubert, F. Rare earth phosphate powders RePO<sub>4</sub>·nH<sub>2</sub>O (Re= La, Ce or Y) - Part I. Synthesis and characterization. *J Solid State Chem* **2004**, *177*, 1302-1311.